Bull. Mater. Sci., Vol. 29, No. 2, April 2006, pp. 107–114. © Indian Academy of Sciences.

Electron density distribution and bonding in ZnSe and PbSe using maximum entropy method (MEM)

K S SYED ALI[†], R SARAVANAN*, S ISRAEL[#] and R K RAJARAM[‡]

Department of Physics, The Madura College, Madurai 625 011, India
[†]Department of Physics, Yadava College, Madurai 625 014, India
[#]Department of Physics, The American College, Madurai 625 002, India
[‡]School of Physics, Madurai Kamaraj University, Madurai 625 021, India

MS received 22 August 2005; revised 14 October 2005

Abstract. The study of electronic structure of materials and bonding is an important part of material characterization. The maximum entropy method (MEM) is a powerful tool for deriving accurate electron density distribution in crystalline materials using experimental data. In this paper, the attention is focused on producing electron density distribution of ZnSe and PbSe using JCPDS X-ray powder diffraction data. The covalent/ionic nature of the bonding and the interaction between the atoms are clearly revealed by the MEM maps. The mid bond electron densities between atoms in these systems are found to be 0·544 e/Å^3 and 0·261 e/Å^3, respectively for ZnSe and PbSe. The bonding in these two systems has been studied using two-dimensional MEM electron density maps on the (100) and (110) planes, and the one-dimensional electron density profiles along [100], [110] and [111] directions. The thermal parameters of the individual atoms have also been reported in this work. The algorithm of the MEM procedure has been presented.

Keywords. MEM; ZnSe; PbSe electronic structure.

1. Introduction

The very important statistical approach of maximum entropy method (MEM), to deal with the various crystallographic problems was introduced by Collins (1982). The maximization of the initial assumed electron density distribution through refinements and the building up of the real electron density distribution have gained momentum nowadays in the analysis of crystal structures and bonding distribution, because the resulting distribution is very precise, highly resolved and very near to the true distribution (Yamamura *et al* 1998; Kajitani *et al* 2001; Saravanan *et al* 2002, 2003; Israel *et al* 2003, 2004).

The precise study of the bonding in materials is always useful and interesting yet no study can reveal exactly the real picture, because no two data sets of a crystalline system are identical. The electron density distribution can be determined experimentally from elaborate X-ray diffraction measurements, and in some cases it can also be calculated from theory. There have been theoretical studies (Narayan and Nityananda 1982; Wilkins *et al* 1983; Navaza 1986; Bricogne and Bayesian 1988) to apply MEM method to problems in crystallography and in particular, to cases in crystallography which involve Fourier technique. The MEM provides us with the least biased deduction, which is compatible with certain given information. The bonding nature and the distribution of electrons in the bonding region can be clearly visualized using this technique (e.g. Livesey and Skilling 1985; Sakata and Kato 1990; De Vries *et al* 1994; Yamamoto *et al* 1996; Israel *et al* 2003, 2004). MEM electron densities are always positive and even with limited number of data, one can evaluate reliable electron densities resembling true densities.

In the present analysis, a study using JCPDS X-ray powder data has been undertaken to determine the electron density, bonding and radii of atoms/ions in ZnSe and PbSe. The systems have been analysed in terms of the structural refinement using JANA 2000, and then the refined structure factors have been utilized for MEM refinements to elucidate the electron density distribution in ZnSe and PbSe. The MEM algorithm has been presented in figure 1, for a clear understanding of the methodology used.

2. Methodology

2.1 *Maximum entropy method*

The exact electron density distribution would be obtained if all of the structure factors were known without any ambiguities. It is, however, impossible to collect exact values of all the structure factors by X-ray diffraction

*Author for correspondence (saragow@dataone.in)

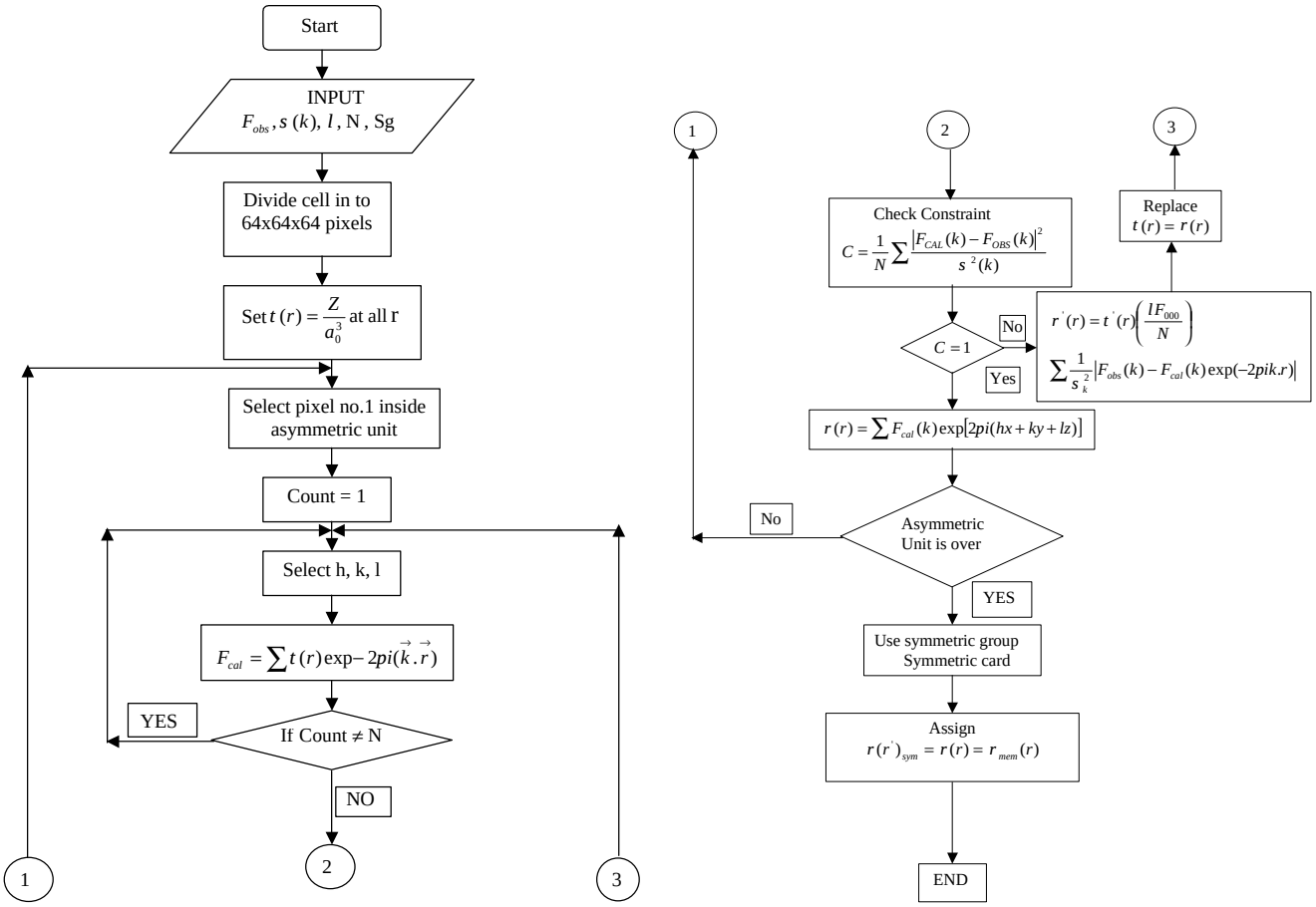

Figure 1. The algorithm of MEM method. (F_{obs} = Observed structure factor; l = Lagrange parameter; $s(k)$ = standard deviation of F_{obs}; Sg = space group; h, k, l = Miller indices; $t(r)$ = prior electron density; $r(r)$ = electron density; $F_{000} = Z$ = number of electrons in the unit cell; a_0 = the cell; constant; F_{cal} = calculated structure factors; N = number of observed reflections).

methods. The numbers of observable structure factors from the experiment are limited and have some errors in them. From the viewpoint of the information theory, it is not appropriate to use an inverse Fourier transform to construct density distribution owing to a limited number of observed structure factors. A question thus arises as to how we should construct the most appropriate density distribution from the limited information obtained experimentally. We must admit that there remain some uncertainties in the results (electron density distribution maps) due to the incompleteness of the experimental observations. The maximum entropy method (MEM) is one of the appropriate methods in which the concept of entropy is introduced to handle the uncertainty properly. The principle of MEM is to obtain an electron density distribution, which is consistent with the observed structure factors and to leave the uncertainties maximum.

MEM was introduced by Gull and Daniel (1978) in radio astronomical image processing. Collins (1982) of Texas A&M Universities, formulated this method for crystallographic applications. He introduced an iterative procedure based on constrained entropy maximization, which constructs the electron density even from very few available imperfect X-ray diffraction data.

The entropy is given by

$$S = -\sum r'(r) \ln \frac{r'(r)}{t'(r)}. \qquad (1)$$

In this expression, $r'(r)$ becomes $t'(r)$ when there is no information. The $r'(r)$ and $t'(r)$ are normalized as

$$\sum r'(r) = 1, \qquad \sum t'(r) = 1.$$

Let the probability, $r'(r)$ and prior probability, $t'(r)$ be related to the actual electron density in a unit cell as,

$$r'(r) = \frac{r(r)}{\sum_r r(r)} \quad \text{and} \quad t'(r) = \frac{t(r)}{\sum_r t(r)},$$

when $r(r)$ and $t(r)$ are the electron and prior electron densities at a certain pixel (r) in a unit cell, respectively.

In the present theory, the actual densities are treated instead of the normalized densities.

The constraint is introduced as

$$C = \frac{1}{N}\sum \frac{\left|F_{\text{cal}}(k) - F_{\text{obs}}(k)\right|^2}{s^2(F_{\text{obs}}(k))},$$

where N is the number of reflections, $s(k)$ the standard deviation of $F_{\text{obs}}(k)$, $F_{\text{obs}}(k)$ the observed structure factor, $F_{\text{cal}}(k)$ the calculated structure factor given by

$$F_{\text{cal}}(k) = V\sum r(r)\exp(2\pi ik.r)\mathrm{d}V, \tag{2}$$

where V is the volume of the unit cell.

This type of constraint is sometimes called a weak constraint, in which the calculated structure factors agree with the observed ones as a whole when C becomes unity.

As can be seen in (2), the structure factors are given by the Fourier transform of the electron density distribution in the unit cell. Equation (2) guarantees that it is possible to allow any kind of deformation of the electron densities in real space as long as information concerning such a deformation is included in the observed data. We use Lagrange's method of undetermined multiplier (l) in order to constrain the function C to be unity while maximizing the entropy.

We then have

$$\begin{aligned} Q &= S - \left(\frac{l}{2}\right)C \\ &= -\sum r'(r)\ln\left(\frac{r'(r)}{t'(r)}\right) - \frac{l}{2N}\sum_k \frac{\left|F_{\text{cal}}(k) - F_{\text{obs}}(k)\right|^2}{s^2(k)}, \end{aligned} \tag{3}$$

and $\mathrm{d}Q/\mathrm{d}r(r) = 0$ yields

$$-\sum_r \frac{r(r)}{\sum r(r)}\frac{t(r)/\sum t(r)}{r(r)/\sum r(r)}\frac{1}{t(r)} - \sum_r \frac{1}{\sum r(r)}\ln\frac{r(r)}{t(r)},$$

$$-\frac{lV^2}{2N}\sum_k \frac{\left|2(r_{\text{cal}} - r_{\text{obs}})e^{-4\pi i\vec{k}.\vec{r}}\right|}{s^2(k)} = 0,$$

$$-\frac{1}{\sum r(r)}\left[1 + \ln\frac{r(r)}{t(r)}\right] - \frac{lV}{N}\sum \frac{\left|F_{\text{cal}}(k) - F_{\text{obs}}(k)e^{-2\pi i\vec{k}.\vec{r}}\right|}{s^2(k)} = 0,$$

using the approximation $\ln x \approx x - 1$.

$$\frac{-r(r)}{t(r)} = \frac{lVz}{N}\sum \frac{\left|F_{\text{cal}}(k) - F_{\text{obs}}(k)e^{-2\pi i\vec{k}.\vec{r}}\right|}{s^2(k)},$$

$$r'(r) = t'(r)\left(\frac{l\,F_{000}}{N}\right)\sum \frac{1}{s^2(k)}\left|F_{\text{cal}}(k) - F_{\text{obs}}(k)e^{-2\pi i\vec{k}.\vec{r}}\right|, \tag{4}$$

where Z is the total number of electrons in the unit cell. Equation (4) cannot be solved as it is, since $F_{\text{obs}}(k)$ is defined on $r(r)$. In order to solve (4) in a simple manner, we introduce the following approximation

$$F_{\text{cal}}(k) = V\sum_r t(r)\exp(-2\pi ik.r)\mathrm{d}V. \tag{5}$$

This approximation can be called the zeroth order single pixel approximation (ZSPA). By using this approximation, the right hand side of (4) becomes independent of $t(r)$ and (4) can be solved in an iterative way starting from a given initial density for prior distribution. For the initial density of prior density, $t(r)$, an uniform density distribution is employed in this work. The choice of prior distribution corresponds to the maximum entropy state among all possible density distributions. It is obvious that there is no prejudice for the initial density. The algorithm of MEM has been given in figure 1.

The maximum entropy method is a statistical deduction that can yield a high resolution density distribution from a limited number of diffraction data without using a structural model. It has been suggested that MEM would be a suitable method for examining electron densities in the outer atomic region, for example, bonding region. It gives less biased information on the electron densities as compared to conventional Fourier synthesis.

2.2 *Structural refinement*

The raw intensity data of ZnSe and PbSe taken from JCPDS data base were corrected for Lorenz-polarization, and multiplicity factor. Other corrections have been given while refining the structure. The structure was refined using JANA 2000, that can refine several structural parameters, the scale, thermal parameters, etc. The results of these refinements are given in table 1. The unit cell of ZnSe and PbSe have been given in figures 2(a) and (b), respectively.

2.3 *MEM refinement*

In the MEM calculations, the unit cell is divided into $64 \times 64 \times 64$ pixels and the initial density at each pixel is fixed uniformly as Z/a_0^3. The electron density is evaluated by carefully selecting the lagrangian multiplier, l, in each case such that the convergence criterion, C, becomes unity after performing minimum number of iterations. The parameters relevant to MEM computations have been given in table 2.

Table 1. Parameters from the least squares refinement using JANA 2000.

Parameter	ZnSe	PbSe
B_{Metal} (Å^2)	1·721 (0·003)	1·542 (0·108)
B_{Se} (Å^2)	0·801 (0·002)	2·149 (0·255)
B_{Metal} (Å^2)	1·020 (0·005)*	2·034**
B_{Se} (Å^2)	0·739 (0·008)*	–
R (%)	1·74	1·95
wR (%)	2·01	2·39

*McIntyre *et al* (1980); **Peng *et al* (1996).

Table 2. Parameters from the MEM analyses.

Parameter	ZnSe	PbSe
Number of cycles	2170	2626
Prior density, $t(r_i)$ (e/Å^3)	1·466	2·020
Lagrange parameter (l)	0·02	0·005
R_{MEM} (%)	3·10	2·45
wR_{MEM} (%)	3·46	2·45
Resolution (Å/pixel)	0·0885	0·0885
Space group	$F-43m$	$Fm3m$

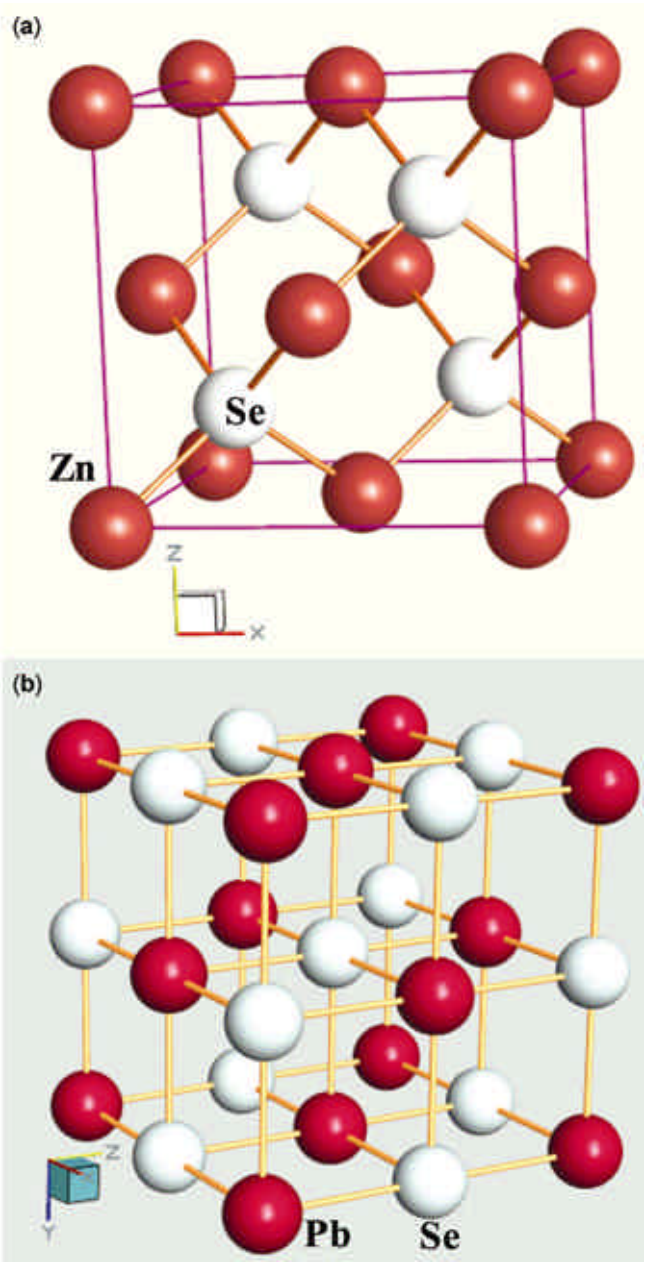

Figure 2. (**a**) Unit cell of ZnSe. Lattice constant of ZnSe is 5·667 Å and (**b**) unit cell of PbSe. Lattice constant of PbSe is 6·124 Å.

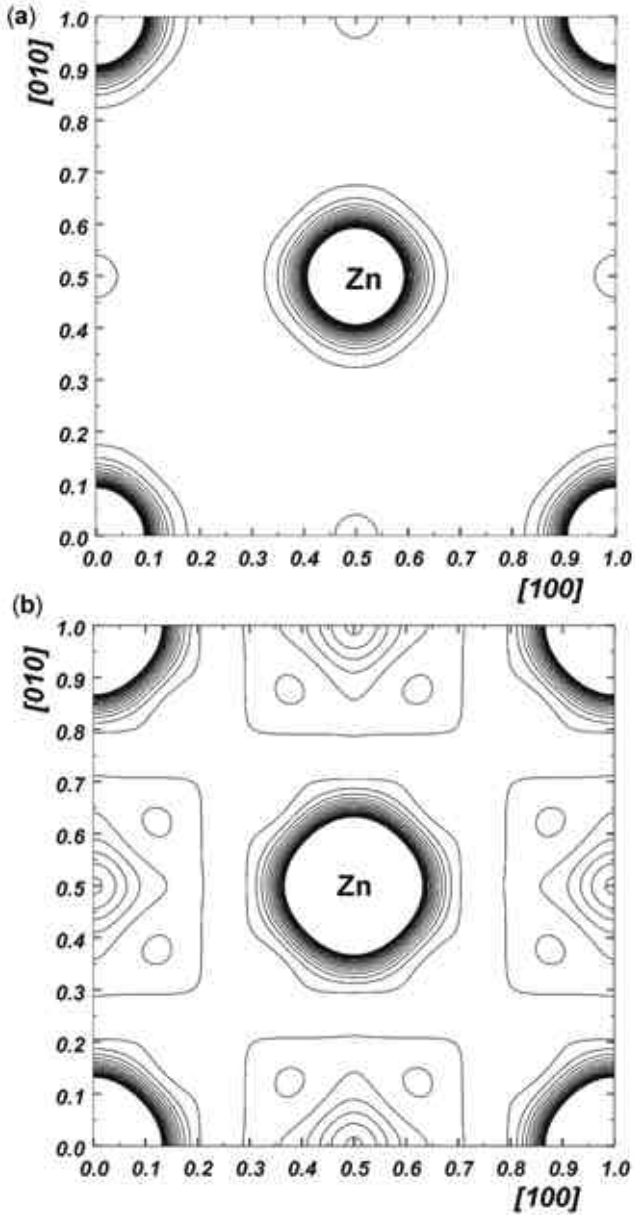

Figure 3. (**a**) High density MEM map of ZnSe on (100) plane. Contour range is from 0·05 e/Å^3 to 10·0 e/Å^3. Contour interval is 0·04975 e/Å^3. The X and Y axes have been normalized to unity by the lattice constant (a = 5·667 Å) and (**b**) low density MEM map of ZnSe on (100) plane. Contour range is from 0·05 e/Å^3 to 2·0 e/Å^3. Contour interval is 0·0975 e/Å^3. The X and Y axes have been normalized to unity by the lattice constant (a = 5·667 Å).

3. Results and discussion

The structure refinement using JANA 2000 gives reasonable values of the Debye-Waller factors for ZnSe obtainable from a powder data set, which can be compared to those of McIntyre *et al* (1980). The reliability indices are also very low indicating the correctness of the refinements.

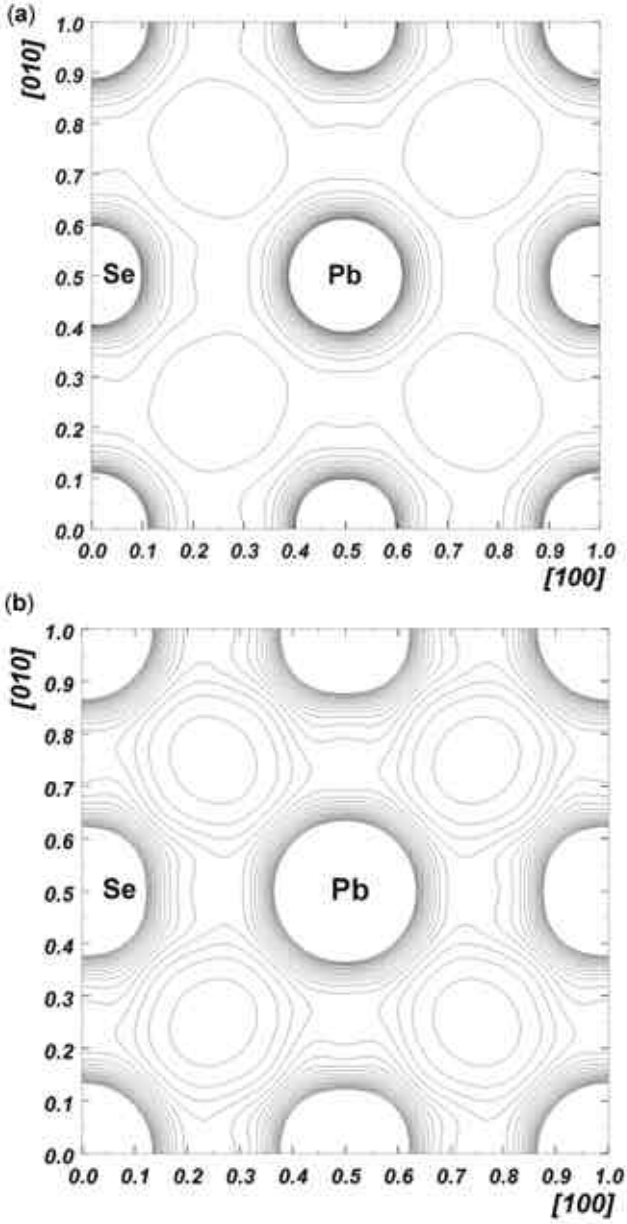

Figure 4. (**a**) High density MEM map of PbSe on (100) plane. Contour range is from 0·00 e/Å^3 to 8·0 e/Å^3. Contour interval is 0·04 e/Å^3. The X and Y axes have been normalized to unity by the lattice constant (a = 6·124 Å) and (**b**) low density MEM map of PbSe on (100) plane. Contour range is from 0·03 e/Å^3 to 3·0 e/Å^3. Contour interval is 0·1485 e/Å^3. The X and Y axes have been normalized to unity by the lattice constant (a = 6·124 Å).

Using the refined structure factor and the phase of each reflection, the MEM calculations were carried out and the parameters have been given in table 2, both for ZnSe and PbSe. The number of refinement cycles is slightly higher for PbSe than ZnSe, probably due to the higher number of

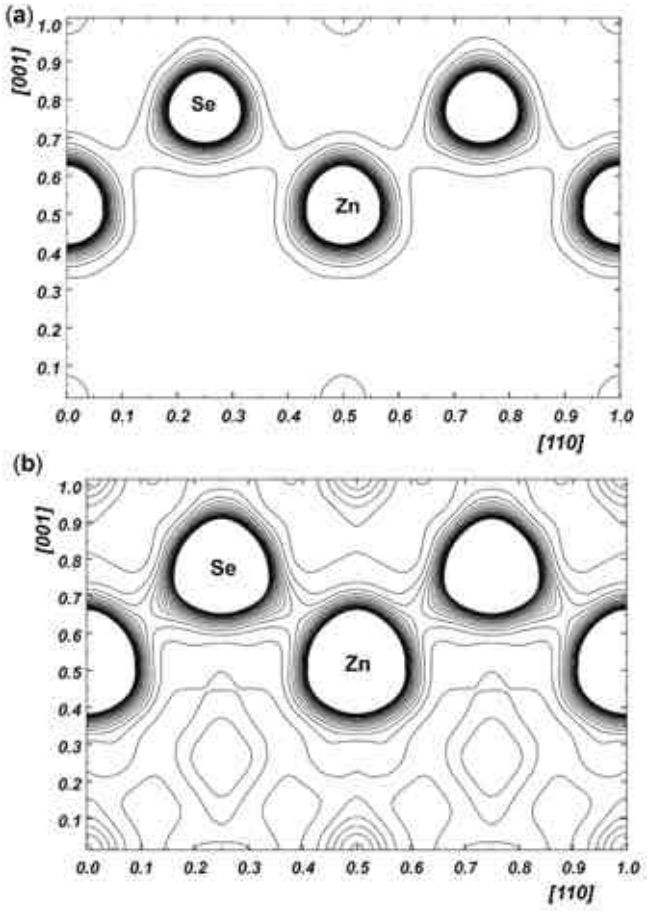

Figure 5. (**a**) High density MEM map of ZnSe on $(1\bar{1}0)$ plane. Contour range is from 0·01 to 9·0 e/Å^3. Contour interval is 0·4495 e/Å^3. The X-axis has been normalized to unity by the lattice constant (a = 5·667 Å). The Y-axis has been normalized to unity by $\sqrt{2}a$ = 8·0131 Å and (**b**) low density MEM map of ZnSe on (110) plane. Contour range is from 0·05 e/Å^3 to 2·0 e/Å^3. Contour interval is 0·0975 e/Å^3. The X-axis has been normalized to unity by the lattice constant (a = 5·667 Å). The Y-axis has been normalized to unity by $\sqrt{2}a$ = 8·0131 Å.

Table 3. The one-dimensional electron density of ZnSe and PbSe along the three directions in the unit cell.

	ZnSe		PbSe	
Direction	Position (Å)	Density (e/Å^3)	Position (Å)	Density (e/Å^3)
[100]	1·859	0·246	1·435	0·665
[110]	2·004	0·274	2·165	0·119
[111]	1·074	0·545	2·652	0·261

electrons in the unit cell, which has been divided into the same number of pixels in both systems. The R_{MEM} and wR_{MEM} values are also low for the two systems and slightly higher for ZnSe than PbSe.

The MEM electron density maps have been constructed on (100) plane of ZnSe and presented in figures 3(a) and (b), for the high and low density regions. Similarly, the high and low density maps on the (100) plane of PbSe have been given in figures 4(a) and (b), respectively.

The maps on the (100) planes can be visualized and interpreted considering the unit cell structures of ZnSe and PbSe given in figures 2(a) and (b), respectively. Figure 3(a) shows perfect spherical nature in the core of Zn atoms. Figure 3(b) shows a similar trend, and since it deals with low density regions also, the edge centres show the electron densities of Zn atoms situated at the centres of the planes perpendicular to the paper. Figure 4(a) for PbSe shows a clear ionic nature of bonding. The electron densities of both Pb and Se are highly resolved resembling only electrostatic attractive/repulsive forces. No symptom of electron sharing is visible. The low-density map shown in figure 4(b) indicates similar electrostatic forces. The electron densities on the $(1\bar{1}0)$ plane of ZnSe show a more covalent type bonding in both figures 5(a) and (b). The tetrahedral symmetry of the structure of ZnSe leads to aspherical inner core electron densities. The electron densities of PbSe on the $(1\bar{1}0)$ plane show clear ionic nature,

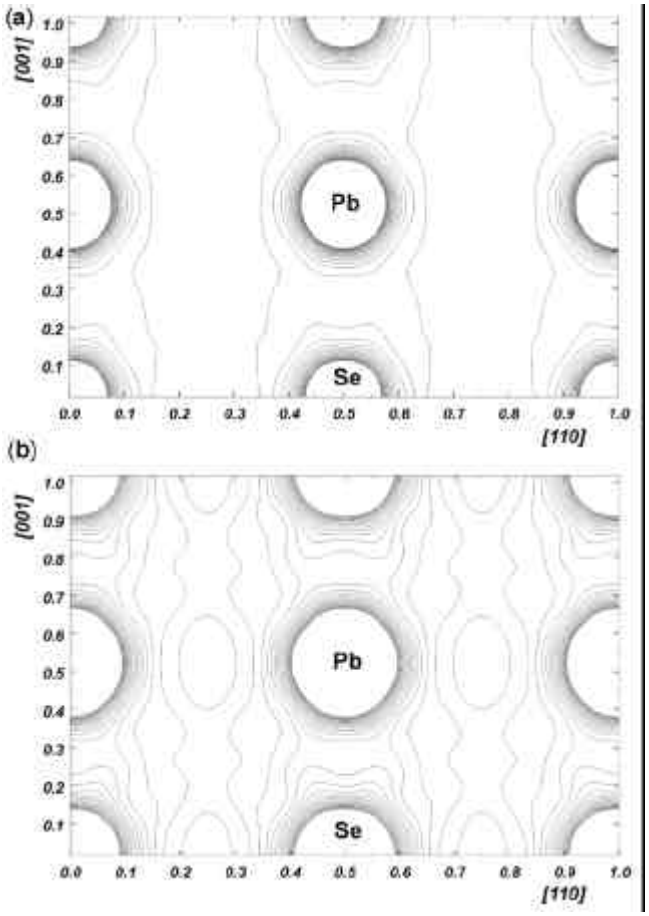

Figure 6. (**a**) High density MEM map of PbSe on $(1\bar{1}0)$ plane. Contour range is from 0·00 to 9·0 e/Å^3. Contour interval is 0·45 e/Å^3. The X-axis has been normalized to unity by the lattice constant (a = 6·124 Å). The Y-axis has been normalized to unity by $\sqrt{2}a = 8 \cdot 6593$ Å and (**b**) low density MEM map of PbSe on $(1\bar{1}0)$ plane. Contour range is from 0·00 e/Å^3 to 3·0 e/Å^3. Contour interval is 0·15 e/Å^3. The X-axis has been normalized to unity by the lattice constant (a = 6·124 Å) The Y-axis has been normalized to unity by $\sqrt{2}a = 8 \cdot 6593$ Å.

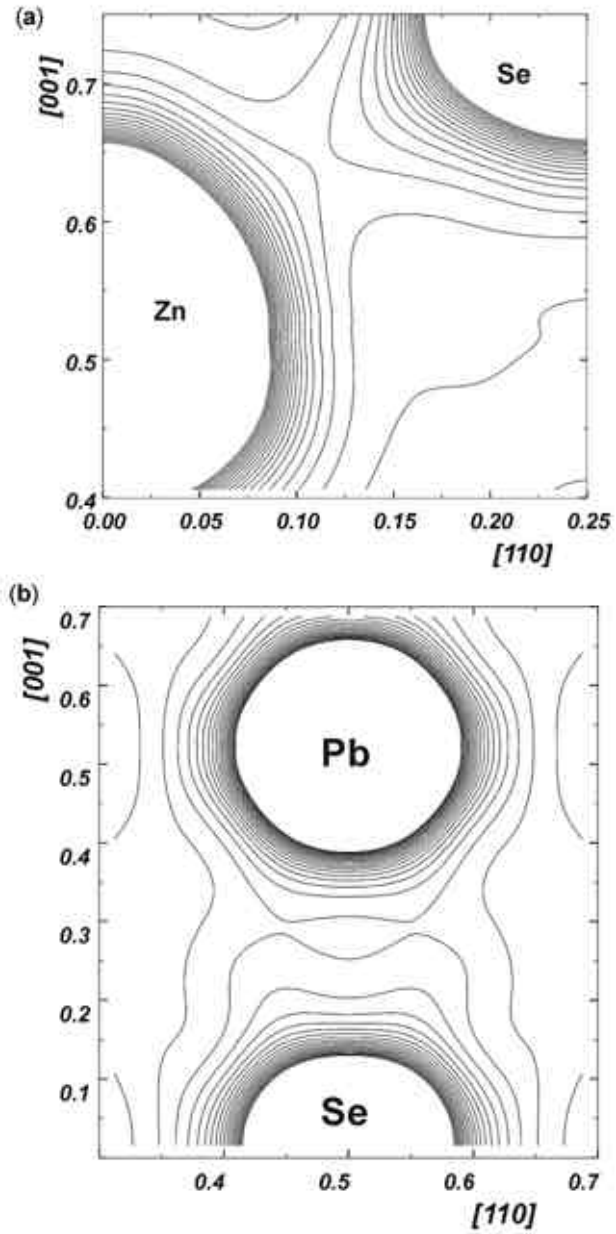

Figure 7. (**a**) MEM map of ZnSe on $(1\bar{1}0)$ plane, with enlarged bonding region. Contour range is from 0·03 e/Å^3 to 2·5 e/Å^3. Contour interval is 0·098 e/Å^3 and (**b**) MEM map of PbSe on $(1\bar{1}0)$ plane, with enlarged bonding region. Contour range is from 0·095 e/Å^3 to 4·0 e/Å^3. Contour interval is 0·195 e/Å^3.

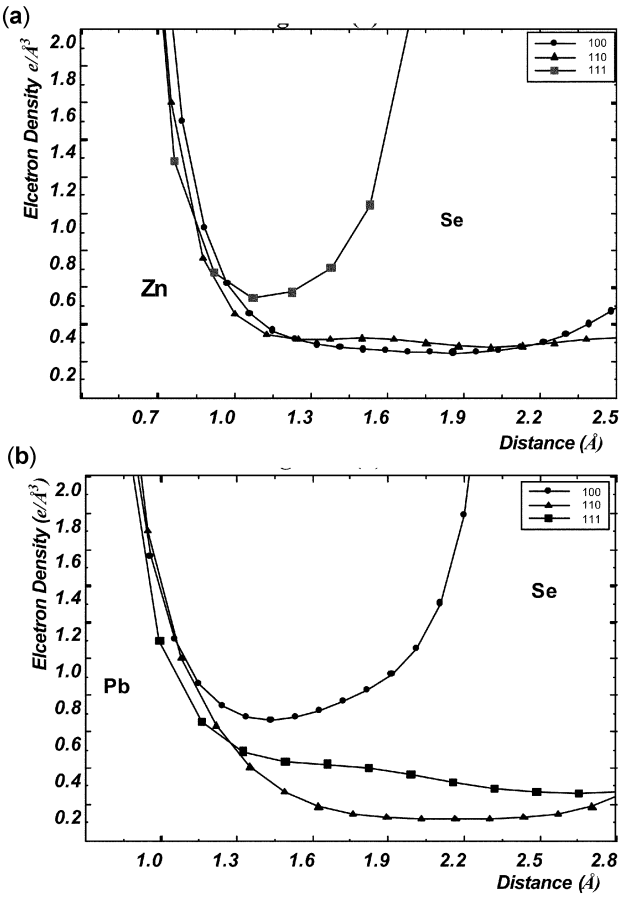

Figure 8. (**a**) One-dimensional variation of electron density along [100], [1$\bar{1}$0] and [111] directions of ZnSe unit cell and (**b**) one-dimensional variation of electron density along [100], [110] and [111] directions of PbSe unit cell.

since, the repulsion of like charges leads to columns of 'void' regions as shown in figure 6 (a) (in the structure of PbSe, like charges on (1$\bar{1}$0) plane are arranged in rows). The high-density map on the (1$\bar{1}$0) plane also shows (figure 6(b)) similar trends of voids between like atoms. Figures 7(a) and (b) show the enlarged portions of bonding region in ZnSe and PbSe, respectively. A more covalent nature in ZnSe and more ionic nature in PbSe are seen from these maps.

The one-dimensional electron densities have been shown in figures 8(a) and (b), respectively, for ZnSe and PbSe along [100], [110] and [111] directions.

The positions of minimum electron densities and the density values have been given in table 3. Along the bonding direction in ZnSe, i.e. [111] direction, the mid-bond densities are found to be 0·545 e/Å^3 at a distance of 1·074 Å. From the cell constant of ZnSe (5·668 Å) (Wyckoff 1960), the inter-atomic distance is found to be 2·454 Å. In the present work, the radius of Zn and Se atoms are found to be 1·074 Å and 1·457 Å, respectively. This gives an inter-atomic distance of 2·531 Å comparable to the value (2·454 Å) calculated from the reported cell constant (Wyckoff 1960).

The value of mid-bond density, 0·545 e/Å^3, along the [1$\bar{1}$1] direction and the two-dimensional MEM maps on (1$\bar{1}$0) planes reveal that ZnSe is possibly more covalent than ionic. The electron density along [100] and [110] directions are relatively low in conformity with the loosely packed structure of ZnSe. (The interaction of atomic charges will be less and hence the electron densities along directions other than bonding are expected to be minimum).

Figure 8(b) of PbSe shows unequal electron densities along the three directions. This is due to the fact that the structure of PbSe is close packed and obviously there will be interactions of close charges, which will be different along different directions. Also, these interactions will affect the bonding charges. Table 3 shows that the mid-bond density along [100] direction is 0·655 e/Å^3 which is higher due to the charge interactions.

The ionic radii of Pb and Se atoms are found to be 1·435 Å and 1·627 Å, respectively. This leads to an experimental bond length of 3·0617 Å, whereas, the bond length calculated from reported cell value is 3·062 Å (Wyckoff 1960), highly comparable to present experimental value. Figure 8(b) shows that due to interactions of charges, the [100] and [110] profile densities vary markedly from each other. The [111] direction shows no hump or non nuclear maximum (NNM), (Iversen *et al* 1995) indicating highly ionic nature of PbSe.

4. Conclusions

A precise analysis has been made using powder data sets on the elucidation of bonding characters and bond lengths using the sophisticated MEM technique. The present report paves the way for the analysis of other important crystalline systems for bonding using limited available information.

Acknowledgements

One of the authors (KSSA) acknowledges the authorities of Yadava College, Madurai, for their encouragement during the course of this research study. (RS) acknowledges the Council of Scientific and Industrial Research, India, for financial support provided through the research project No.: 03(0949)/02/EMR-II.

References

Bricogne G and Bayesian A 1988 *Acta Crystallogr.* **A44** 212
Collins D M 1982 *Nature* **298** 49
De Vries R Y, Brils W J and Feil D 1994 *Acta Crystallogr.* **A50** 383
Gull S F and Daniel G J 1978 *Nature* **272** 686

Israel S, Saravanan R, Srinivasan N and Rajaram R K 2003 *J. Phys. Chem. Solids* **64** 43

Israel S, Saravanan R and Rajaram R K 2004 *Physica* **B349** 390

Iversen B B, Larsen F K, Souhassou M and Takata M 1995 *Acta Crystallogr.* **A51** 580

Kajitani T, Saravanan R, Ono Y, Ohno K and Isshiki M 2001 *J.Cryst. Growth* **229** 130

Livesey A K and Skilling J 1985 *Acta Crystallogr.* **A41** 113

McIntyre G J, Moss G and Barnea Z 1980 *Acta Crystallogr.* **A36** 482

Narayan R and Nityananda R 1982 *Acta Crystallogr.* **A38** 122

Navaza J 1986 *Acta Crystallogr.* **A42** 212

Peng L M, Ren G, Dudarev S L and Whelan M J 1996 *Acta Crystallogr.* **A52** 257

Sakata M and Kato A 1990 *Acta Crystallogr.* **A46** 263

Saravanan R, Israel S, Swaminathan S, Kalidoss R and Muruganantham M 2002 *Cryst. Res. Technol.* **37** 1310

Saravanan R, Ono Y, Ohno Isshiki M, Ohno K and Kajitani T 2003 *J. Phys. Chem. Solids* **64** 51

Vaclac Petricek and Michal Dusek Lukas Palatinus JANA 2000 The crystallographic computing system, Institute of Physics, Academic of sciences of the Czech Republic. http://www-x-ray.fzu.cz/JANA/JANA 2000/html

Yamamura S, Takata M, Sakata M and Suguwara Y 1998 *J. Phys. Soc. Japan* **67** 4124

Yamamoto K, Takahashi Y, Ohshima K, Okamura F B and Yukino K 1996 *Acta Crystallogr.* **A52** 606

Wilkins S W, Varghese J N and Lehmann M S 1983 *Acta Crystallogr.* **A39** 47

Wyckoff R W G 1960 *Crystal structures* (London: Inter-Science Publishers) Vol. I